

DVCS Simulation with SoLID-SIDIS configuration

Zhihong Ye
Duke University

April 8, 2015

Abstract

This report quickly summaries my study of the DVCS simulation with the SoLID-SIDIS configuration. Results are preliminary and will be constantly updated.

1 Monte Carlo Simulation Data

The simulated events were generated with Carlos's generator. In general, it is straightforward to generate an event with random combination of kinematic variables, Q^2 , x , t and ϕ , and calculate the energy, momentum and angles of both the electron and photon. I implemented a slightly wider SoLID-SIDIS acceptance to judge whether both particles can be accepted by SoLID or not. In the generator, the ranges of kinematic variables I used to randomly generate events are given as:

$$\begin{aligned} Q_{min}^2 &= 1.0 \text{ GeV}^2, Q_{max}^2 = 13.0 \text{ GeV}^2, x_{min} = 0.1, x_{max} = 0.8, \\ t_{min} &= -2.0 \text{ GeV}^2, t_{max} = 0.0 \text{ GeV}^2, \text{ and } \phi_{min} = 0^\circ, \phi_{max} = 360^\circ. \end{aligned} \quad (1)$$

We can define a phase-space factor which will be used later when evaluating the rate:

$$PSF \equiv \Delta Q^2 \Delta x \Delta t \Delta \phi = (Q_{max}^2 - Q_{min}^2) \times (x_{max} - x_{min}) \times (t_{max} - t_{min}) \times (\phi_{max} - \phi_{min}). \quad (2)$$

Events were simulated two energy settings, $E_{beam}=8.8$ GeV or 11 GeV, and in each setting, the total number of generated events is:

$$N_{gen} \equiv 20,000,000. \quad (3)$$

Only events that are in the SoLID acceptance can be stored in a ROOT file.

In SoLID-SIDIS configuration, we detect electrons and photons at both the large-angle electromagnetic-calorimeter (LAEC) and the forward-angle electromagnetic-calorimeter (FAEC). The coverage of the detectors coded in the generator is:

$$\begin{aligned} 6^\circ < \theta_e < 26^\circ, 0^\circ < \phi_e < 360^\circ, 0.5 \text{ GeV} < P_e < 11 \text{ GeV}, \\ 6^\circ < \theta_\gamma < 26^\circ, 0^\circ < \phi_\gamma < 360^\circ, 0 \text{ GeV} < P_\gamma < 11 \text{ GeV}. \end{aligned} \quad (4)$$

The more accurate and complicated SoLID-SIDIS acceptance was applied afterward. We extracted the acceptance profiles of electrons and neutral particles (e.g. photons) from our SoLID GEANT4 simulation which contains the magnetic filed, the realistic geometries and materials of the magnet and all detectors. The acceptance profiles are basically the 2-D histograms of momentum .vs. polar angle (i.e., P_e .vs. θ_e) without weighted by cross sections. Simply speaking, the acceptance value is equal to one if the particle is within the acceptance. For electrons, the acceptance has a distribution from 0 to 1 at the edge of the phase space and also depends on the momentum and angles. Because we will detect both electron and photon and form the coincidence, the overall acceptance for one event is given as:

$$A = (ele_accpt_fa + ele_accpt_la) \times (pho_accpt_fa + pho_accpt_la), \quad (5)$$

where $ele(pho)_accpt_fa(la)$ is the acceptance value of an electron (photon) at FAEC (LAEC).

2 VGG Cross Section Model

(Note: More introduction about VGG will be added later.) The VGG model is able to provide the BH+DVCS cross section with the known inputs of Q^2 , x , t , and ϕ . In the double polarized case, the code computes four cross section values at the same time, i.e. σ^{++} , σ^{+-} , σ^{-+} , and σ^{--} , where first and second superscript (\pm) gives the polarization direction of the beam and the target, respectively. The unit of the cross section is in $nb \cdot GeV^{-4} \cdot rad^{-1}$ and was later converted into $cm^2 \cdot GeV^{-4} \cdot rad^{-1}$.

	Min	Max	Step
Q^2	1 GeV^2	9 GeV^2	1 GeV^2
x	0.05	0.75	0.05
t	-2.5 GeV^2 or t_{max}	0 GeV^2 or t_{min}	0.05 GeV^2
ϕ	0°	360°	15°

Table 1: Ranges and steps for physics variables when calculating cross sections with VGG

The VGG code runs very slow so it is not practical to compute the cross sections in an event-by-event base. As shown in Table 1, after determining the range and step of each variable, I created a 4D grid where in each grid point the four cross section values were computed. The polarization of the electron beam is always longitudinal (L), while there are three target polarization directions, i.e. longitudinal, transverse on x (Tx) and transverse on y (Ty). Hence there are three double-spin combinations, LL, LTx and LTy. With two energy settings, there are 6 grids I created.

With these grids, I am able to search the cross section values for each simulated event created by the generator. Given an event with known values of these four variables, I searched which two grid points each variable falls into, and used the linear relationship to calculate the “actual” cross section value with the known values on the two grid points. For example, if the value of ϕ is between ϕ_i and ϕ_{i+1} , the correction is given as:

$$cor(\phi) = 1 + \frac{\phi - \phi_i}{\phi_{i+1} - \phi_i} \frac{\sigma_{i+1} - \sigma_i}{\sigma_i}. \quad (6)$$

Hence, there are four corrections ($cor(Q^2)$, $cor(x)$, $cor(t)$, $cor(\phi)$) when searching cross sections for each event. A C++ script was written to perform searching and apply corrections. A random test with several events was proceeded to compare the difference between the values computed directly by VGG and searched by the script. The results show less than 0.5% deviation but a more careful check can be done later.

3 Integrated Rate

	TGVKelly		VGG	
	8.8 GeV	11 GeV	8.8 GeV	11 GeV
	Single Rates (Hz)			
e- (FAEC)	117.64	63.42	259.26	144.67
e- (LAEC)	4.25	3.60	11.09	6.73
γ (FAEC)	80.37	55.09	182.56	162.27
γ (LAEC)	8.48	5.80	125.30	115.54
	Coincidence Rates (Hz)			
e-(FAEC)+ γ (FAEC+LAEC)	40.12	19.00	144.48	82.28
e-(LAEC)+ γ (FAEC+LAEC)	2.08	1.50	6.25	3.94

Table 2: Ranges and steps for physics variables when calculating cross sections with VGG

We will perform the exclusive DVCS measurement and hence it requires the coincident trigger of electrons and photons. The integrated rates given below are not corrected by the beam and

target polarization, target dilution and so on. They are not corrected by the detector efficiency as well (which is about 85%). It will just represent what we can detect at the trigger level.

The rates are calculated with the simulated events weighted by their total cross sections and acceptances. In Carlos' generator, the TGVKelly model was used to compute the unpolarized cross sections. I used these values to evaluate the rates. After generating the cross section grids, I redid the calculation with the cross sections from VGG. In the Table 2, the VGG model gives the coincidence rates which are a factor of 3 larger than the ones from TGVKelly. The biggest difference is the single photon rates at LAEC. I am looking for the reason now.

4 Beam Time, Target, etc

Currently I assume the DVCS experiment will be in the run group of the SoLID-SIDIS and hence share the beam time of the approved experiments. The approved beam time of two energy settings are:

$$T_{8.8\text{GeV}} = 21 \text{ days}, T_{11\text{GeV}} = 48 \text{ days}. \quad (7)$$

In the SoLID-SIDIS experiments, we will use transverse polarized ^3He target (neutron) and longitudinal polarized NH_3 target (proton). In this study, I only evaluated the transverse case. With 15 nA beam current, the neutron luminosity in the ^3He target is:

$$L = 1 \times 10^{36} \text{ cm}^{-2} \text{ s}^{-1}. \quad (8)$$

The beam polarization and the ^3He polarization are set to be 100% and 60%, respectively. The effective neutron in ^3He is known to be close to 86.5%, and the dilution is estimated to be 20%. The total detector efficiency is assumed to be 85%

5 Data Binning and Projections

The binning was performed for each energy setting (8.8 GeV or 11 GeV) and each target polarization setting (LL, LT_x or LT_y). The simulated data were binned in 4-dimensions with a sequence of Q^2 , x , t and ϕ , where the size of each bin for each variable is determined by the array given in Eq. 9. Hence, there are 5 Q^2 bins, 5 x bins, 6 t bins and 12 ϕ bins.

$$\begin{aligned} Q^2[6] &= \{1, 2, 3, 4, 5, 7\}, \\ x[6] &= \{0.1, 0.2, 0.3, 0.4, 0.5, 0.7\}, \\ t[7] &= \{-2, -0.7, -0.5, -0.4, -0.3, -0.2, -0.1\} \\ \phi[13] &= \{0, 30, 60, 90, 120, 150, 180, 210, 240, 270, 300, 330, 360\} \end{aligned} \quad (9)$$

In each bin, the number of events is calculated from the total simulated events by applying cuts on the corresponding ranges of the four variables. For instance, for the bin, (1,2,3,4), the number of event is computed with the cut:

$$(1 \leq Q^2 < 2 \ \&\& \ 0.2 \leq x < 0.3 \ \&\& \ -0.5 \leq t < -0.4 \ \&\& \ 90 \leq \phi < 120 \ \&\& \ W > 2).$$

To get the raw counts in each bin, we also need to apply the weight of the cross section and acceptance value for each event in the bin:

$$N_{raw} = \sum_{i \in bin} \sigma_i^{sum} \cdot A_i, \quad (10)$$

where the cross section σ_i^{sum} is the sum of σ_i^{++} , σ_i^{+-} , σ_i^{-+} , σ_i^{--} , obtained by the grid searching script. A_i is given by Eq. 5. The number of normalized by the phase-space, total generated events, acceptance, beam-time and target luminosity, and so on, from Eq. 2, 3, 5, 7, and 8:

$$N = N_{raw} \cdot PSF/N_{gen} \cdot T_{8.8/11\text{GeV}} \cdot L \cdot \epsilon_{eff} \cdot (P_{beam} \cdot P_{target} \cdot Dilution \cdot N_{eff})^2, \quad (11)$$

where P_{beam} and P_{target} are 100% and 60%, respectively. $Dilution$ is 20%, the effective neutron factor, N_{eff} , is 86.5%, and the detector efficiency, ϵ_{eff} , is 85%. The relative statistical error for each bin can then be evaluated:

$$\Delta \equiv \delta N/N = 1.0/\sqrt{N}. \quad (12)$$

The mean cross section values in each bin were evaluated, given as $\bar{\sigma}_i^{++}$, $\bar{\sigma}_i^{+-}$, $\bar{\sigma}_i^{-+}$, and $\bar{\sigma}_i^{--}$. One can obtain the beam-spin asymmetry (A_{BS}), target-spin asymmetry (A_{TS}) and double-spin asymmetry (A_{DS}) from different combination of these four cross sections:

$$\begin{aligned} A_{BS} &= \frac{1}{4}(\bar{\sigma}_i^{++} + \bar{\sigma}_i^{+-} - \bar{\sigma}_i^{-+} - \bar{\sigma}_i^{--}), \delta A_{BS} = A_{BS} \cdot \Delta \cdot P_{target} \\ A_{TS} &= \frac{1}{4}(\bar{\sigma}_i^{++} - \bar{\sigma}_i^{+-} + \bar{\sigma}_i^{-+} - \bar{\sigma}_i^{--}), \delta A_{TS} = A_{TS} \cdot \Delta \cdot P_{beam} \\ A_{DS} &= \frac{1}{4}(\bar{\sigma}_i^{++} - \bar{\sigma}_i^{+-} - \bar{\sigma}_i^{-+} + \bar{\sigma}_i^{--}). \delta A_{DS} = A_{DS} \cdot \Delta \end{aligned} \quad (13)$$

The statistical errors of these asymmetries are propagated from Eq. 12. Note that from the beam (target)-spin asymmetry, the statistical error was corrected by the target (beam) polarization, since the number of count in each bin was corrected by both polarizations, as shown in Eq. 11.

6 Compton Form Factor Projections

I am still looking for a script to fit the Compton form factors (CFF) from the asymmetry distributions as a function of ϕ in each (Q^2, x, t) combination. I will update the CFF projections later.

7 Missing Mass and Background

In the current study, we assume that we will only detect scattered electrons and real photons from the DVCS reaction, and reconstruct the neutron missing mass to select the real events. The resolutions of measuring the momentum (or energy) and angles for electrons are determined by the GEM tracking reconstruction which is designed to achieve the following resolutions:

$$\delta P_e/P_e \sim 2\%, \delta\theta_e \sim 0.6 \text{ mrad}, \delta\phi_e \sim 5 \text{ mrad},$$

and the resolutions for photons are determined by the cluster reconstruction of ECs (FAEC and LAEC). The angular resolutions are determined by the EC position resolutions and the target vertex position (δz_{vertex}) given by the electron tracking reconstruction. The current design can reach the accuracy as:

$$\delta x_{EC} = 1 \text{ cm}, \delta y_{EC} = 1 \text{ cm}, \delta z_{vertex} = 0.5 \text{ cm}.$$

The energy resolution of ECs is designed to be $\sim 5\%$.

The neutron missing mass spectra at the 8.8 GeV and 11 GeV setting are given in Fig. 1 and Fig 2, after implemented the detector resolutions. In the same figures, the π^0 background was also included. However, the π^0 events were not weighted by their cross sections due to the lack of a working cross section model. This part is needed to be updated.

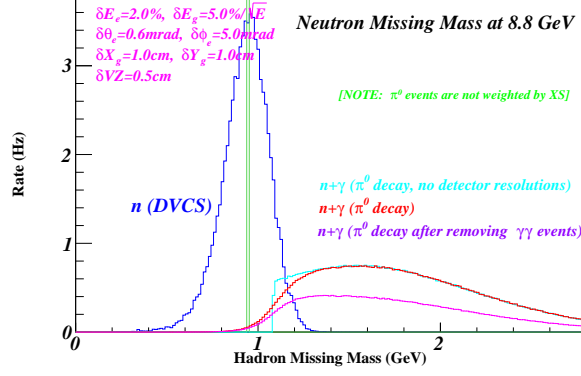


Figure 1: The neutron missing mass at $E_{beam} = 11 \text{ GeV}$ (blue line). The detector resolutions were considered in the calculation. The π^0 background (red line) was normalized by comparing with the 6 GeV Hall-A DVCS results. We also evaluate the π^0 combination (magenta line) after removing these events which we can detect both π^0 decayed photons. An updated version will be available once we have the $e^- n \rightarrow \pi^0$ exclusive cross section model.

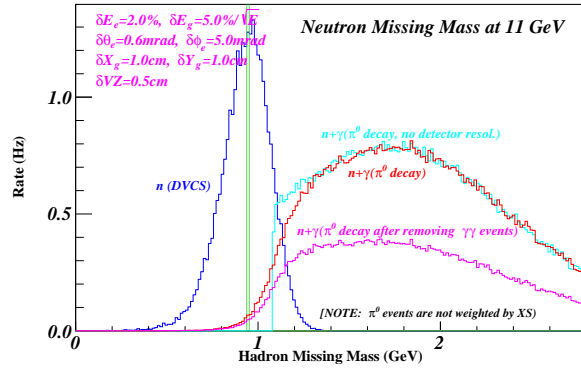


Figure 2: The neutron missing mass at $E_{beam} = 11 \text{ GeV}$ (blue line). The detector resolutions were considered in the calculation. The π^0 background (red line) was normalized by comparing with the 6 GeV Hall-A DVCS results. We also evaluate the π^0 combination (magenta line) after removing these events which we can detect both π^0 decayed photons. An updated version will be available once we have the $e^- n \rightarrow \pi^0$ exclusive cross section model.